

Recognition-Directed Supramolecular Assemblies of Metal Complexes of Terpyridine Derived Ligands with Self-Complementary Hydrogen Bonding Sites

Ulrich Ziener,^[a] Esther Breuning,^[a] Jean-Marie Lehn,^{*[a]} Elina Wegelius,^[b] Kari Rissanen,^[b] Gerhard Baum,^[c] Dieter Fenske,^[c] and Gavin Vaughan^[d]

Abstract: The synthesis and X-ray structures of three metal complexes with terpyridine-derived ligands that contain amino-pyrimidine and amino-pyrazine moieties are presented. They have been designed in view of directing their self-assembly into specific supramolecular arrays through molecular recognition interactions. The solid-state structures indeed reveal extensive hydrogen-bonded networks. The Co complex **4a** with PF₆⁻ counterions builds a two-dimensional infinite interwoven grid through strong double hydrogen bonds ($d(\text{N-H-N}) = 2.918\text{--}3.018\text{ \AA}$) between the amino groups and the N atoms of the rings, with all H-bonding sites saturated. Changing the anions to BF₄⁻ in **4b** leads to a similar infinite but partially broken grid with a quarter of the H-bonding sites unsaturated ($d(\text{N-H-N}) = 2.984\text{--}3.206\text{ \AA}$). In the case of the Zn complex

12 with triflate anions, half of the hydrogen bonds are formed. Only one of the two orthogonal ligands has hydrogen bonds ($d(\text{N-H-N}) = 3.082, 3.096\text{ \AA}$) to the neighbouring complexes and thus builds linear, supramolecular, polymeric chains. These structural differences are mainly attributed to crystal-packing effects caused by the different anions. The data presented here may also be regarded as a prototype for the generation of organised arrays through sequential self-assembly processes.

Keywords: coordination chemistry · crystal engineering · hydrogen bonds · ligand design · supramolecular chemistry

Introduction

In the past few years much effort has been devoted to the construction of new supramolecular assemblies through metal coordination, for example, grids, cages, racks and helices.^[1] Additional hydrogen bonding allows further design of such assemblies and is used as a tool in crystal engineering.^[2] Metal complexes that are connected by hydrogen bonds possess the capability to form ordered supramolecular arrays of metal

ions with interesting redox activity or magnetic properties, which could lead towards molecular storage devices. The motifs employed so far for hydrogen bonding together with metal complexes in a designed fashion are, for example, carboxamides,^[3–5] oximes,^[4] carboxylic acids^[4] and functionalised *N*-heteroaromatics.^[6–8] The use of complementary hydrogen-bonding units provides a further tool for crystal engineering of interest to materials science and molecular electronics.^[2, 6, 9] By adequate positioning of hydrogen-bond donor (D) and acceptor (A) sites a large number of complementary systems with singly and multiply bonded systems has been developed.

Here we report on the synthesis and structures of terpyridine-derived ligands **3** and **11** and their Co and Zn complexes **4** and **12**. Bipyridine and terpyridine ligands form a large variety of metal complexes that display a range of interesting physico-chemical properties and have been extensively studied. For future applications it is therefore of special interest to design ways for the controlled arrangement of such complexes into supramolecular arrays of defined architectures. In the present case, the terpyridine unit has been fitted with amino-pyrimidine and amino-pyrazine units. In contrast to ligands and metal complexes which exhibit hydrogen bonds only accidentally to solvent molecules and/or counterions, the

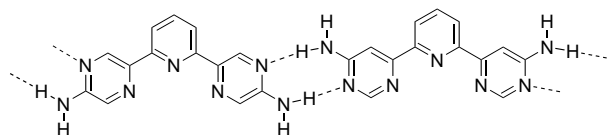
[a] Prof. Dr. J.-M. Lehn, Dr. U. Ziener, E. Breuning
Laboratoire de Chimie Supramoléculaire, ISIS
Université Louis Pasteur
4 rue Blaise Pascal, 67000 Strasbourg (France)
Fax: (+33)388-411-020
E-mail: lehn@chimie.u-strasbg.fr

[b] E. Wegelius, Prof. Dr. K. Rissanen
Department of Chemistry, University of Jyväskylä
PO Box 35, 40351 Jyväskylä (Finland)

[c] G. Baum, Prof. Dr. D. Fenske
Institut für Anorganische Chemie, Universität Karlsruhe,
Engesserstrasse, Geb.-Nr. 30.45, 76128 Karlsruhe (Germany)

[d] Dr. G. Vaughan
European Synchrotron Radiation Facility, ESRF
BP220, 38043 Grenoble Cedex (France)

compounds **3** and **11** allow the formation of well-defined, double hydrogen bonds by self-complementarity. They should also be capable of building heterocomplementary interaction patterns between amino-pyrimidine and amino-pyrazine groups, thus forming two-dimensional polymers connected by A/D:D/A H-bond arrays. Crystallisation of the metal complexes of these heterocomplementary terpyridine-like ligands $[M^1(\mathbf{3})_2]$ and $[M^2(\mathbf{11})_2]$ with each other, should generate an alternating sequence of the two metals M^1 and M^2 in infinite two-dimensional sheets in a chess-board-like manner (Scheme 1).



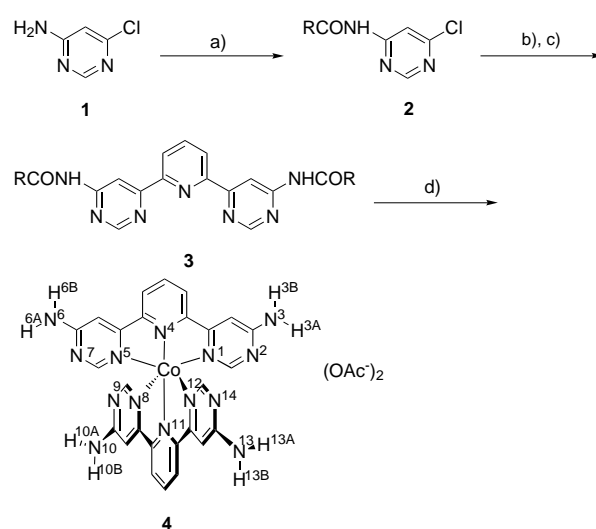
Scheme 1. Terpyridine-like ligands in the metal-complex conformation capable of forming complementary hydrogen bonds.

Results and Discussion

Synthesis of ligands **3 and **11** and of complexes **4** and **12**:** The synthesis of the ligand **3** and the Co complex **4** is schematically outlined in Scheme 2.

Ligand **3** is built up from pyrimidine and pyridine units and synthesised by stannylation and a subsequent Stille cross-coupling reaction. We introduced a long-chain acyl group as

Abstract in German: *Im Folgenden werden die Synthesen und Einkristallstrukturen von drei Metallkomplexen mit terpyridin-ähnlichen Liganden, die Aminopyrimidin bzw. Aminopyrazin enthalten, vorgestellt. Die Liganden wurden gezielt entworfen, um durch molekulare Erkennung die Selbstassoziation der Komplexe in eine spezifische supramolekulare Ordnung zu lenken. Tatsächlich zeigen die Festkörperstrukturen über Wasserstoffbrücken ausgedehnte Netzwerke. Der Co-Komplex **4a** mit $PF_6^{<M^->-}$ -Gegenionen bildet ein zweidimensional-unendliches, verwobenes Gitter. Dabei liegen starke zweifache Wasserstoffbrücken ($d(N-H-N) = 2.918-3.018 \text{ \AA}$) zwischen den Aminogruppen und den Ringstickstoffatomen unter Ab-sättigung aller Wasserstoffbrücken vor. Durch Austausch der Anionen gegen $BF_4^{<M^->-}$ (**4b**) gelangt man zu einer ähnlichen unbegrenzten, allerdings teilweise aufgebrochenen Gitterstruktur, bei der ein Viertel der Wasserstoffbrücken nicht abgesättigt ist ($d(N-H-N) = 2.984-3.206 \text{ \AA}$). Im Falle des Zn-Komplexes **12** mit Triflatanionen zeigt sich, dass nur noch die Hälfte der Wasserstoffbrücken ausgebildet wird. Nur einer der beiden orthogonalen Liganden ist über zweifache Wasserstoffbrücken ($d(N-H-N) = 3.082, 3.096 \text{ \AA}$) mit Nachbarkomplexen verknüpft und bildet somit lineare, supramolekulare polymere Ketten. Diese strukturellen Unterschiede werden im Wesentlichen auf Kristallpackungseffekte durch die unterschiedlichen Anionen zurückgeführt. Die hier vorgestellten Ergebnisse können auch als Prototyp für die Erzeugung organisierter Strukturen durch schrittweise Selbstassoziationsprozesse aufgefasst werden.*



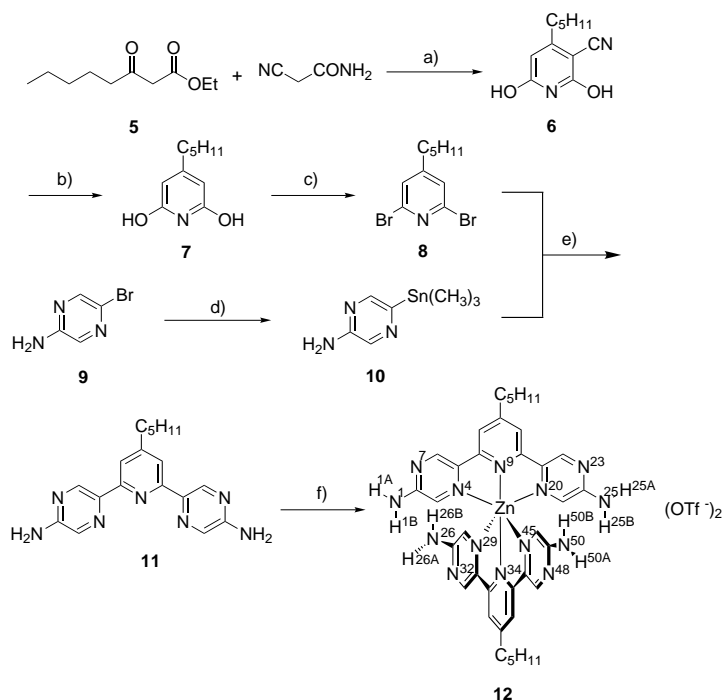
Scheme 2. Synthesis of ligand **3** and Co complex **4**. a) $CH_3(CH_2)_4COCl$, pyridine, $CHCl_3$; b) Me_6Sn_2 , $[Pd(PPh_3)_4]$, toluene; c) 2,6-dibromopyridine, $[Pd(PPh_3)_4]$, toluene; d) $Co(OAc)_2 \cdot 2H_2O$, MeOH.

solubilising substituent on the amino group in **1**, since the poor solubility of the unprotected compound was an obstacle to the following Pd-catalysed stannylation and Stille reaction. This protection group was removed in one step during the complexation reaction with cobalt acetate. The coordination bond of the pyrimidine N atom to the Co atom in the *para* position to the amide group weakens the amide bond sufficiently to be split off by methanol (as solvent) by heating under reflux without any catalyst. The removal of the acyl substituent was necessary for the formation of the desired H-bonds.

The reaction of **3** with $Co(OAc)_2 \cdot 4H_2O$ in MeOH can be observed in the 1H NMR spectrum. The diamagnetic spectrum of **3** is completely changed upon complexation. It exhibits four peaks for H_{arom} , thus maintaining the C_{2v} symmetry of the ligand with paramagnetic chemical shifts up to $\delta = 90.5$. Due to line broadening, coupling information is lost and no assignment of the peaks can be performed.

The synthesis of **11** is similar to that of **3** (Scheme 3). Owing to changed reactivity and poor solubility of intermediate compounds we could not follow exactly the same route as for the synthesis of **3**. We introduced a permanent alkyl substituent in the 4-position of the pyridine moiety in analogy to a known strategy.^[10, 11] Ligand **11** is soluble enough for the complexation reaction and forms readily the Zn complex **12** with $Zn(OTf)_2$ in acetonitrile as indicated by 1H NMR spectroscopy. The C_{2v} symmetry of the ligand is maintained, and though no clear assignment of the peaks for the two $H_{pyrazine}$ atoms can be made, both are shifted upfield by $\Delta\delta = 1$ ppm.

Crystal structures of complex **4:** After anion exchange with NH_4PF_6 , we were able to obtain single crystals of the Co complex **4a** that were suitable for analysis by X-ray crystallography. The crystal structure reveals that **4a** forms an infinite two-dimensional gridlike structure in the solid state. The terpyridine-derived ligands are connected by intermo-



Scheme 3. Synthesis of ligand **11** and Zn complex **12**. a) Piperidine, cyanacetamide, MeOH; b) H₂SO₄, H₂O; c) POBr₃; d) Me₆Sn₂, [Pd(PPh₃)₄], toluene; e) [Pd(PPh₃)₄], toluene; f) Zn(OTf)₂·H₂O, CH₃CN.

lecular double H-bonds between the amino groups and the noncoordinating pyrimidine N atoms (Figure 1). Recently, the common characteristics of solid-state structures of terpyridine-metal complexes [M(terpy)₂]^{z+} were reviewed.^[12] Most often, an interdigitation of the outer pyridine rings is found, due to face-to-face and edge-to-face interactions between the pyridine moieties. In our structure, this feature is absent because of the establishment of strong hydrogen bonds that take over the generation of the network (Table 1). Due to the self-complementarity of the H-bonding functionalities of the ligands in **4a**, the complexes show a sinusoidal arrangement which causes an interwoven network in both directions without hydrogen-bonding interactions in the direction perpendicular to the plane of the grid.

The Co–N bond lengths of **4a** are in the typical range for [Co(terpy)₂]²⁺ complexes (Table 1). The absolute Co–N bond lengths in such complexes strongly depend on the spin state of the Co²⁺ ion and, therefore, on subtle lattice forces caused by the counter ions and lattice solvent molecules.^[13] The X-ray structures of only two [CoL₂]²⁺ complexes with substituted terpyridine ligands and PF₆⁻ as anions have been described.^[13] The Co–N bond lengths to the central pyridine rings of these mainly low-spin complexes ($d(\text{Co}-\text{N}_{\text{central pyridine}}) = 1.904, 1.942 \text{ \AA}$ and $1.866, 1.922 \text{ \AA}$, respectively) are approximately 0.2 Å shorter than in **4a** (Table 1). Therefore we assume that the Co^{II} in **4a** is predominantly high-spin in agreement with [Co(terpy)₂](ClO₄)₂ ($d(\text{Co}-\text{N}_{\text{central pyridine}}) = 2.019, 2.026 \text{ \AA}$, ca. 70% high-spin state).^[14]

The lengths of the hydrogen bonds N–H–N are between 2.918 and 3.028 Å with angles between 161° and 172°. Compared with purely organic hydrogen-bonded 4-amino-

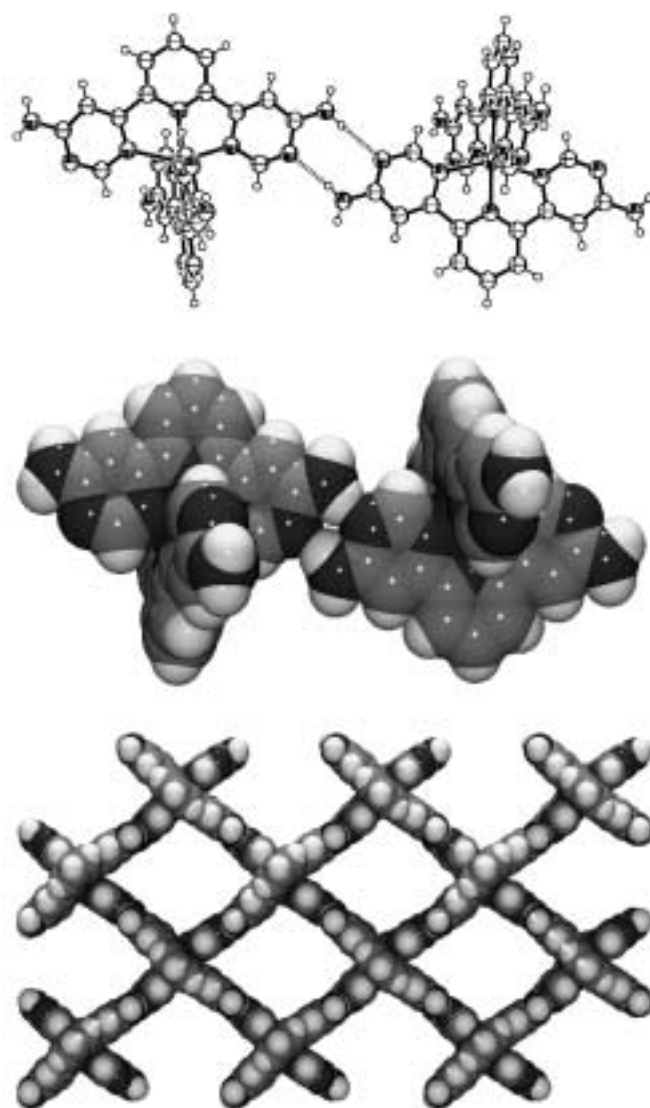


Figure 1. X-ray structure of complex **4a**. Top and middle: Two molecules with hydrogen bonding contacts (ORTEP-style, space-filling representation, respectively). Bottom: Crystal packing (space-filling representation).

Table 1. Selected averaged bond lengths [Å] and angles [°] for complex **4a** and for each of the two molecules in the asymmetric unit of complex **4b**.

bond/angle ^[a]	4a	4b	
Co–N _{ax}	2.074	1.898	2.059
Co–N _{eq}	2.151	1.969	2.123
N _{ax} –Co–N _{ax}	177.5	178.6	176.3
N _{eq} –Co–N _{eq}	150.7	163.1	152.9
N–(H)–N	2.918–3.028	2.984–3.206	
N–H–N	161.2–172.4	165.3–173.2	

[a] ax: Co–N bonds to the pyridine moiety, eq: Co–N bonds to the pyrimidine moiety.

pyrimidine units, which exhibit the same double hydrogen-bond features as **4a**, they prove to be strong H-bonds (4-amino-5-phenyl-pyrimidine as adduct with vanilline: $d(\text{N-H-N}) = 3.051(3) \text{ \AA}$, $\text{angle}(\text{N-H-N}) = 171(2)^\circ$;^[15] 4-amino-2,6-dichloro-pyrimidine: $d(\text{N-H-N}) = 3.09 \text{ \AA}$ ^[16]). Probably, the metal coordination in *para* position of the amino group increases the hydrogen donor ability.

Anion exchange of **4** with NH_4BF_4 led us to the BF_4^- complex **4b**. Attempts were made to co-crystallise **4b** with an Fe complex that contained amino-pyrazine in order to construct the afore-mentioned network in a chess-board-like fashion by heterocomplementary hydrogen bonding (Scheme 1). X-ray analysis revealed that single crystals, which were of sufficient quality, from these experiments contained only pure **4b**. In the solid-state structure of **4b**, the principal features of **4a** are kept, exhibiting a two-dimensional infinite grid by hydrogen bonding in two directions. In contrast to **4a**, however, the H-bonds of **4b** are only fully saturated in one direction, whereas in the perpendicular direction, half of the bonds remain unsaturated; this leads to a partially broken grid structure (Figure 2). The asymmetric unit of **4b** is composed

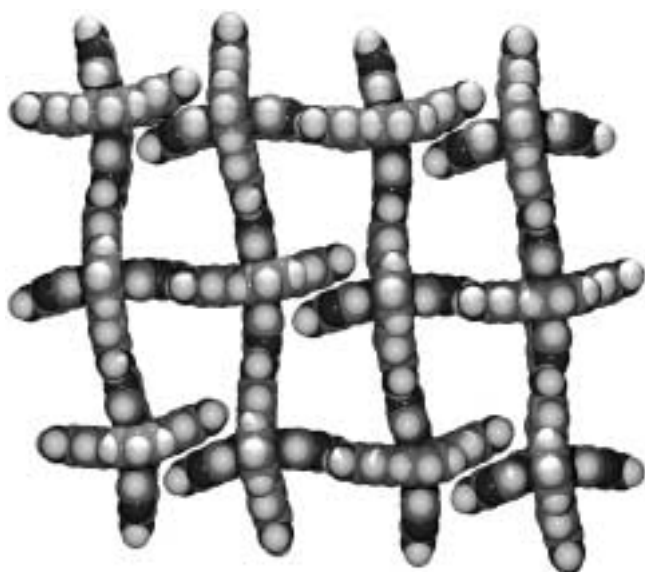


Figure 2. X-ray structure of complex **4b**, space-filling representation of the crystal packing.

of two molecules of the complex, which differ in Co–N bond lengths and N–Co–N angles quite markedly (Table 1). It is striking that the average Co–N bond lengths of one complex are significantly shorter than those of the other ($d(\text{Co–N})_{\text{avg}} = 1.945$ and 2.102 Å). Additionally, there are five anions found in the asymmetric unit instead of the four expected for two Co^{II} cations. On comparison with literature values $\{[\text{Co}^{\text{II}}(\text{terpy})_2](\text{ClO}_4)_2\}$: $d(\text{Co–N})_{\text{avg}} = 2.030$ (axial), 2.137 Å (equatorial); $[\text{Co}^{\text{III}}(\text{terpy})_2]\text{Cl}_3$: $d(\text{Co–N})_{\text{avg}} = 1.859$ (ax.), 1.928 Å (equatorial)},^[17] these two features lead to the deduction that the Co centres of **4b** are in the average oxidation state 2.5, built from one Co^{II} and one Co^{III} cation. As the ^1H NMR spectrum of **4b** did not show any significant differences to **4a**, though a change in the oxidation state is expected to influence the chemical shift, we assume that the oxidation process occurred during the process of crystallisation. Electrochemical investigations indeed revealed that **4b** has a low oxidation potential, which gives a hint to a facilitated oxidation ($E_{1/2} = -0.18$ V vs. ferrocene as internal standard in $\text{CH}_3\text{CN}/\text{MeOH}$, $0.1\text{M } n\text{Bu}_4\text{NPF}_6$; $[\text{Co}^{\text{III}}(\text{terpy})_2]/[\text{Co}^{\text{II}}(\text{terpy})_2]$: $E_{1/2} = +0.243$ V vs. SCE in CH_3CN , $0.1\text{M } n\text{Bu}_4\text{NPF}_6$).^[18] The influence of the Fe complex on the oxidation process in

this co-crystallisation experiment is unclear, but further attempts to obtain single-crystals from solutions of the pure Co complex **4b** failed.

With a deviation from the ideal plane up to about 1 Å, the ligands in **4b** are more bent than in **4a**. This distortion of the ligands might cause weaker H-bonds in **4b** ($d(\text{N–H–N}) = 2.984$ – 3.206 Å, $d_{\text{avg}} = 3.075$ Å). The angles N–H–N (165.3° to 173.2°) in **4b** are similar to those in **4a**. Whereas in **4a** two PF_6^- anions fit quite well in the opposite corners of each mesh within the grid, the BF_4^- anions in **4b** are smaller and form additional (N)–H–F–(B) H-bonds with the unsaturated amino groups, thus partially breaking up the grid. Though the hydrogen bonds dominate the solid-state structure, they are only weak forces and might be overwhelmed by crystal packing effects caused by different anions.

Crystal structure of complex 12: The crystal structure of complex **12** (Figure 3) is markedly different from that of complexes **4a** and **4b**. The gridlike arrangement is no longer present, and H-bonding between the amino groups and the noncoordinating N atoms of the pyrazine ring is maintained in only one direction; this results in one-dimensional polymers of H-bonded bis(terpyridine)-like complexes. The parallel alignment of the infinite chains in a layered structure is similar to the grid layers in the structures described above. The amino groups of the ligands that are not involved in the polymeric chains are hydrogen bonded to solvent molecules and anions.

Though no structures of pure $[\text{Zn}(\text{terpy})_2]^{2+}$ complexes are known, the Zn–N bond lengths in **12** (Table 2) are comparable with the values of those found in complexes in which the ligands are substituted at the central pyridine ring by dihydroxyphenyl and dimethoxyphenyl groups.^[13]

The H-bond lengths N–H–N in **12** are 3.082 and 3.096 Å and the angles are 171° and 169° , respectively (Table 2). The difference of the bond lengths to purely organic hydrogen-bonded amino-pyrazine is small.^[19] The amino groups and the heteroaromatic rings of one ligand in **12** are almost coplanar, but the planes of H-bonded ligands of two neighbouring complexes exhibit a dihedral angle of approximately 63° . Thus, they are quite different from the above-mentioned complexes. We assume that the lower connecting efficiency of the self-complementary hydrogen bonds of **12** relative to those in **4a** and **4b** is mainly caused by the different space requirement of the triflate counterion, which is nonspherical and bigger than PF_6^- and BF_4^- , thus changing the crystal packing dramatically. Additionally, triflate competes as the better hydrogen-bonding acceptor more strongly with the N–(H)–N bonds. Hence, perpendicular to the H-bonded polymers, the molecules are staggered and resemble the common structural feature of bis(terpyridine) metal complexes,^[12] although no direct face-to-face or edge-to-face interactions are evident (see above). Further crystallisation experiments with different solvents and spherical anions gave only crystals of low quality.

Conclusion

The synthesis and solid-state structure of three $[\text{M}(\text{L})_2]^{2+}$ complexes ($\text{M} = \text{Co}, \text{Zn}$) with two terpyridine-derived ligands

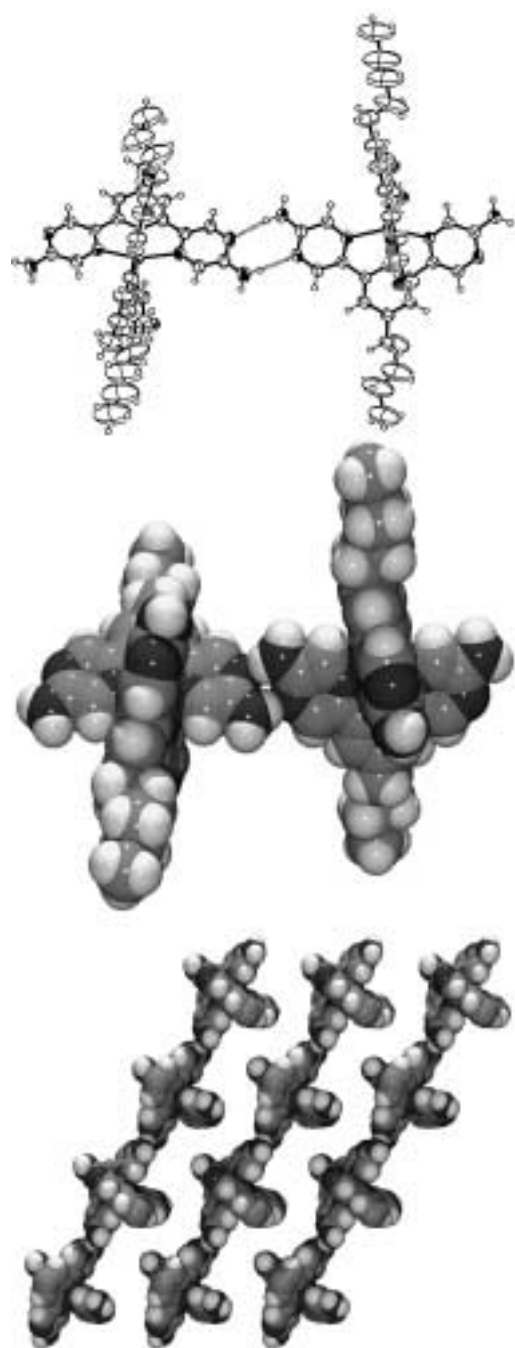


Figure 3. X-ray structure of complex **12**. Top and middle: Two molecules with hydrogen-bonding contacts (ORTEP-style; space-filling representation, respectively). Bottom: Crystal packing (space-filling representation; the alkyl chains are omitted for clarity).

Table 2. Selected averaged bond lengths [Å] and angles [°] of complex **12**.

bond/angle ^[a]	12
Zn–N _{ax}	2.060
Zn–N _{eq}	2.195
N _{ax} –Zn–N _{ax}	173.8
N _{eq} –Zn–N _{eq}	151.6
N–(H)–N	3.082; 3.096
N–H–N	168.5; 171.3

[a] ax: M–N bonds to the pyridine moiety, eq: M–N bonds to the pyrazine moiety.

(L) are presented. These ligands are designed to form double, self-complementary H-bonds. The Co complex **4a**, with PF₆[−] as counterion, has full saturation of the H-bonding sites of amino-pyrimidine in a well-designed, infinite grid structure. BF₄[−] as counterions in **4b** changes the structure of the two-dimensional infinite grid. H-bonds are maintained in one direction, whereas in the other only pairwise H-bonds are formed leaving the other half unsaturated. In **4b**, half of the Co atoms are oxidised to Co^{III}, thus increasing the number of counterions compared with **4a**. The spatial requirement of these anions might additionally affect the crystal structure. In contrast, Zn complex **12** as a triflate salt exhibits only one-dimensional polymeric chains. We assume that apart from the weaker H-bonding ability of the pyrazine moiety and the steric requirements of the alkyl chains in **12**, the different counterions are mainly responsible for the different structures with incomplete H-bonding networks. The subtle interplay between the structure-defining hydrogen bonding and crystal packing, caused by different anions, leads for the three complexes **4a**, **4b** and **12** to three different structures. Besides the self-complementarity of the ligands, as described in the present complexes, the H-bonding amino-pyrimidine and amino-pyrazine units should also be capable of forming heterocomplementary hydrogen-bonding motifs by two-point interaction. Mixed complexes of this type are especially interesting as they would allow the self-assembly of grids with alternating metals M¹ and M² in a layered, chess-board-like fashion. They may represent approaches to locally addressable, inorganic, molecular storage devices. Further experiments for the cocrystallisation of complementary hydrogen bonds between **4** and **12** are underway in order to explore this possibility of precise metal-ion positioning through suitable manipulation of molecular recognition features.

Data such as these presented here are of significance for the development of sequential self-assembly processes as a powerful route for generating large, organised supramolecular arrays of functional components.

Experimental Section

General: 4-Amino-6-chloro-pyrimidine (**1**),^[20] ethyl-3-oxo-hexanoate (**5**)^[21] and 2-bromo-5-amino-pyrazine (**9**)^[22] were prepared according to the literature. Toluene was dried by heating under reflux with sodium under argon for several hours. The other reagents and solvents were used without further purification. The NMR data were obtained on a Bruker AC200 instrument at 200.1 MHz (¹H) and 50.2 MHz (¹³C), calibrated against the solvent signal ([D₆]DMSO: ¹H NMR: δ = 2.50; ¹³C NMR: δ = 39.9; CDCl₃: ¹H NMR: δ = 7.26; ¹³C NMR: δ = 77.0; [D₄]methanol: ¹H NMR: δ = 3.31; [D₃]acetonitrile: ¹H NMR: δ = 1.94) and the chemical shifts are given in ppm. IR data were collected on Perkin Elmer 1600 series FTIR spectrometer and are reported in cm^{−1}.

4-Pentylcarboxamido-6-chloro-pyrimidine (2): Compound **1** (3.11 g, 24 mmol) and hexanoic acid chloride (9.69 g, 72 mmol) were mixed in CHCl₃ (120 mL). After addition of pyridine (20 mL), an orange solution formed which was stirred at room temperature for 2.5 d. The mixture was poured into water, the phases separated and the aqueous phase extracted with CH₂Cl₂ (3 × 50 mL). The combined organic extracts were dried over MgSO₄, and the solvent was removed to yield a slowly crystallising oil. Chromatographic purification on alumina with CHCl₃ afforded a white solid. Yield: 4.52 g (83 %); m.p. 84 °C; ¹H NMR (CDCl₃): δ = 0.85 (m, 3H; CH₃), 1.30 (m, 4H; 2CH₂), 1.68 (m, 2H; CH₂), 2.42 (t, ³J = 8 Hz, 2H; CH₂),

8.24 (d, $^4J = 1$ Hz, 1H; H² or H⁵), 8.59 (d, $^4J = 1$ Hz, 1H; H² or H⁵), 8.64 (s, 1H; NH); ¹³C NMR (CDCl₃): $\delta = 172.7, 162.3, 158.1, 157.9, 109.8, 37.6, 31.1, 24.6, 22.2, 13.7$ cm⁻¹; MS (FAB): m/z : 228.2 [M+H]⁺; IR (KBr): $\tilde{\nu} = 3250, 3131, 2954, 2859, 1723, 1583, 1560, 1487, 1352, 1303, 1252, 1153, 1080, 991, 872, 746, 562$; elemental analysis calcd (%) for C₁₀H₁₄ClN₃O (227.7): C 52.75, H 6.20, N 18.45; found C 52.69, H 6.18, N 18.55.

2,6-Bis(4'-pentylcarboxamidopyrimid-6'-yl)pyridine (3):^[23] Compound **2** (474 mg, 2.1 mmol), hexamethyldistannane (720 mg, 2.2 mmol) and [Pd(PPh₃)₄] (92 mg, 0.08 mmol) were dissolved in toluene (5 mL), flushed with Ar and heated under reflux for 3 h. 2,6-Dibromopyridine (213 mg, 0.9 mmol), [Pd(PPh₃)₄] (35 mg, 0.03 mmol) and toluene (1 mL) were added to the black mixture. The mixture was kept under reflux for 18 h, the solvent was removed, and the residue washed once with diethyl ether and three times with methanol/acetone (1:1 v/v) to afford an off-white powder. Yield: 253 mg (53%); m.p. 258 °C; ¹H NMR ([D₆]DMSO): $\delta = 0.88$ (m, 3H; CH₃), 1.32 (m, 4H; 2CH₂), 1.62 (m, 2H; CH₂), 2.48 (t, $^3J = 8$ Hz, 2H; CH₂), 8.22 (t, $^3J = 8$ Hz, 1H; H⁴), 8.52 (d, $^4J = 1$ Hz, 2H; H², H⁵), 9.01 (s, 2H; H² or H⁵), 9.07 (s, 2H; H² or H⁵), 10.98 (s, 2H; NH₂); ¹³C NMR ([D₆]DMSO): $\delta = 173.2, 162.7, 159.2, 158.2, 153.7, 139.0, 123.3, 105.5, 36.0, 30.6, 24.1, 21.8, 13.7$; MS (FAB): m/z : 462.3 [M+H]⁺; IR (KBr): $\tilde{\nu} = 3226, 2924, 2854, 1702, 1676, 1591, 1546, 1516, 1396, 1378, 1247, 1178, 1096, 993, 902, 830, 775, 633, 570$ cm⁻¹; elemental analysis calcd (%) for C₂₅H₃₁N₇O₂ (461.6): C 65.06, H 6.77, N 21.24; found C 65.01, H 6.65, N 21.34.

Cobalt(II) complex 4: Ligand **3** (10.0 mg, 21.7 μ mol) and Co(OAc)₂ · 4H₂O (2.7 mg, 10.8 μ mol) were mixed in MeOH (1 mL) and heated under reflux for 17 h to form a red-brown suspension. The mixture was centrifuged and the complex precipitated from the supernatant by adding Et₂O. The brown precipitate was centrifuged, washed after 30 min with Et₂O and dried in vacuo to yield a red-brownish powder. Yield: 5.0 mg (65%); ¹H NMR ([D₆]methanol): $\delta = 10.8, 62.8, 65.3, 90.5$; MS (FAB): m/z : 648.3 [M - OAc]⁺, 589.3 [M - 2OAc]⁺; IR (KBr): $\tilde{\nu} = 3318, 3177, 2924, 1642, 1612, 1571, 1485, 1405, 1344, 1011$ cm⁻¹; high-resolution MS (FAB): calcd (m/z) for C₂₆H₂₂CoN₁₄ [M - 2OAc]: 589.148385; found 589.146700.

3-Cyano-2,6-dihydroxy-4-pentyl-pyridine (6): Compound **5** (2.11 g, 11.3 mmol), cyanacetamide (0.95 g, 11.3 mmol) and piperidine (0.95 g, 11.3 mmol) in MeOH (3 mL) were heated under reflux for 24 h. The solvent was evaporated, and the residue was dissolved in hot water. The product was precipitated by addition of concentrated HCl, filtered, washed with ice water and CHCl₃ and dried in vacuo to give **6** as a white powder. Yield: 912 mg (39%); m.p. 205–210 °C (decomp); ¹H NMR ([D₆]DMSO): $\delta = 0.86$ (t, $^3J = 5.8$ Hz, 3H; CH₃), 1.28 (m, 4H; 2CH₂), 1.54 (q, $^3J = 6.7$ Hz, 2H; CH₂), 2.50 (t, $^3J = 7.3$ Hz, 2H; CH₂), 5.57 (s, 1H; H⁵); ¹³C NMR ([D₆]DMSO): $\delta = 164.2, 162.1, 161.3, 117.0, 91.8, 88.2, 34.0, 30.6, 28.4, 21.7, 13.7$; MS (FAB): m/z : 207.2 [M+H]⁺; IR (KBr): $\tilde{\nu} = 2932, 2223$ (CN), 1603, 1498, 1359, 1297, 635 cm⁻¹; high resolution MS (FAB): calcd (m/z) for C₁₁H₁₅N₂O₂ [M+H]: 207.11335; found 207.113841.

2,6-Dihydroxy-4-pentylpyridine (7): A mixture of compound **6** (5.93 g, 28.8 mmol), concentrated H₂SO₄ (12 mL) and water (10 mL) was heated under reflux for 5 h. The mixture was cooled with ice and neutralised with solid NaHCO₃. The precipitate was filtered, washed with water and Et₂O and dried in vacuo to give a mixture of **7** and of the free acid, which was not decarboxylated (0.90 g, 4.0 mmol). The mixture was used without further purification for the next reaction step. Yield: 3.74 g (72%); ¹H NMR ([D₆]DMSO): $\delta = 0.86$ (t, $^3J = 6.7$ Hz, 3H; CH₃), 1.28 (m, 4H; 2CH₂), 1.49 (q, $^3J = 6.1$ Hz, 2H; CH₂), 2.32 (t, $^3J = 7.3$ Hz, 2H; CH₂), 5.57 (s, 2H; H³, H⁵); MS (FAB): m/z : 182.2 [M+H]⁺; IR (KBr): $\tilde{\nu} = 3364, 3048, 2930, 1651, 1516, 1450, 1304, 1208, 994, 632$ cm⁻¹; high resolution MS (FAB): calcd (m/z) for C₁₀H₁₆NO₂ [M+H]: 182.11810; found 182.118064.

2,6-Dibromo-4-pentyl-pyridine (8): Compound **7** (1.44 g, 7.93 mmol) and POBr₃ (7.26 g, 25.33 mmol) were ground and melted together at 140–150 °C for 1 h. After cooling, the mixture was quenched with water, neutralised with solid NaHCO₃ and extracted with CHCl₃ (3 × 100 mL). The combined organic phases were washed with water (1 × 100 mL) and dried over MgSO₄, and the solvent was evaporated. The product was purified by column chromatography on silica with hexane/EtOAc (9/1, v/v) to give **8** as a colourless oil. Yield: 1.42 g (58%); ¹H NMR (CDCl₃): $\delta = 0.88$ (t, $^3J = 6.4$ Hz, 3H; CH₃), 1.29 (m, 4H; 2CH₂), 1.59 (q, $^3J = 7.6$ Hz, 2H; CH₂), 2.53 (t, $^3J = 7.3$ Hz, 2H; CH₂), 7.24 (s, 2H; H³, H⁵); ¹³C NMR ([D₆]DMSO): $\delta = 157.20, 140.53, 127.04, 34.51, 31.11, 29.55, 22.56, 13.82$ cm⁻¹; MS (FAB): m/z : 308.0 [M+H]⁺; IR (film): $\tilde{\nu} = 3067, 2929,$

2859, 1576, 1530, 1465, 1371, 1322, 1224, 1150, 1087, 982, 762; elemental analysis calcd (%) for C₁₀H₁₃Br₂N (307.0): C 39.12, H 4.27, N 4.56; found C 39.21, H 4.30, N 4.41.

2-Trimethylstannyl-5-amino-pyrazine (10):^[23] Compound **9** (1.00 g, 5.75 mmol), hexamethyldistannane (2.07 g, 6.32 mmol) and [Pd(PPh₃)₄] (199 mg, 0.17 mmol) were combined in toluene (20 mL), flushed with Ar and heated under reflux for 1 h. The solvent was evaporated, and the residue purified by column chromatography on silica with hexane/EtOAc (1:3, v/v) to give **10** as a pale yellow powder. Yield: 923 mg (62%); m.p. 102 °C (decomp); ¹H NMR (CDCl₃): $\delta = 0.33$ (s, 9H; 3CH₃), 4.42 (brs, 2H; NH₂), 7.98 (d, $^3J = 1.8$ Hz, 1H; H³ or H⁶), 8.20 (d, $^3J = 1.5$ Hz, 1H; H³ or H⁶); ¹³C NMR ([D₆]DMSO): $\delta = 153.5, 152.3, 147.7, 134.9, -9.6$; MS (FAB): m/z : 260.0 [M+H]⁺; IR (KBr): $\tilde{\nu} = 3318, 3156, 2975, 2909, 1652, 1565, 1535, 1453, 1377, 1203, 1080, 1021, 892, 766, 524$ cm⁻¹; elemental analysis calcd (%) for C₇H₁₃N₃Sn (257.9): C 32.60, H 5.08, N 16.29; found C 32.80, H 4.99, N 16.30.

2,6-Bis(5-aminopyrazin-2-yl)-4-pentyl-pyridine (11): Compound **10** (200 mg, 0.78 mmol), compound **8** (107 mg, 0.35 mmol) and [Pd(PPh₃)₄] (24 mg, 0.021 mmol) in were combined in toluene (8 mL), flushed with Ar (for some minutes) and heated under reflux for 17 h. The solvent was evaporated, and the residue purified by column chromatography on silica with EtOAc/EtOH (4:1, v/v) to give **11** as a yellow powder. A sample for microanalysis was obtained by boiling the powder in hexane/EtOAc (5/2, v/v). Yield: 88 mg (73%); m.p. 207 °C; ¹H NMR ([D₆]DMSO): $\delta = 0.88$ (t, $^3J = 7.0$ Hz, 3H; CH₃), 1.37 (m, 4H; 2CH₂), 1.74 (q, $^3J = 7.6$ Hz, 2H; CH₂), 2.73 (t, $^3J = 7.3$ Hz, 2H; CH₂), 4.73 (brs, 4H; 2NH₂), 7.97 (s, 2H; H³, H⁵), 8.03 (d, $^3J = 1.2$ Hz, 2H; H³, H^{3'} or H⁶, H^{6'}), 9.23 (d, $^3J = 1.5$ Hz, 2H; H³, H^{3'} or H⁶, H^{6'}); ¹³C NMR ([D₆]DMSO): $\delta = 155.9, 154.0, 152.8, 140.4, 138.3, 130.8, 117.0, 34.8, 30.8, 29.5, 21.8, 13.8$; MS (FAB): m/z : 336.2 [M+H]⁺; IR (KBr): $\tilde{\nu} = 3324, 3173, 2928, 2852, 1633, 1601, 1535, 1487, 1430, 1387, 1019, 878$ cm⁻¹; elemental analysis calcd (%) for C₁₈H₂₁N₇ (335.4): C 64.46, H 6.31, N 29.23; found C 64.32, H 6.24, N 29.21.

Zinc(II) complex 12: Ligand **11** (5.0 mg, 15.0 μ mol) and Zn(OTf)₂ · H₂O (2.84 mg, 7.5 μ mol) in CH₃CN (1 mL) were stirred at room temperature for 2.5 h. The solvent was evaporated to give **12** as a pale yellow powder in quantitative yield. ¹H NMR ([D₃]acetonitrile): $\delta = 0.99$ (t, $^3J = 6.8$ Hz, 6H; CH₃), 1.51 (m, 8H; 4CH₂), 2.98 (t, $^3J = 7.3$ Hz, 4H; CH₂), 5.79 (s, 8H; 4NH₂), 6.98 (d, $^5J = 1.3$ Hz, 4H; H³, H^{3'} or H⁶, H^{6'}), 8.20 (s, 4H; H³, H⁵), 9.03 (d, $^3J = 1.3$ Hz, 4H; H³, H^{3'} or H⁶, H^{6'}); MS (FAB): m/z : 883.4 [M - OTf]⁺, 737.4 [M - 2OTf]⁺; IR (film): $\tilde{\nu} = 3222, 1678, 1441, 1248, 1172, 1030, 640$ cm⁻¹; high resolution MS (FAB): calcd (m/z) for C₃₈H₄₂F₆N₁₄O₆S₂Zn [M-OTf]: 883.252859; found 883.250545.

X-ray crystallographic data for Co complex 4a · PF₆⁻: Single crystals of complex **4a** (PF₆⁻ salt) were obtained by dissolving **4** in MeOH and adding NH₄PF₆ in MeOH. The resulting mixture was evaporated to dryness, washed twice with water and the residue dried in vacuo. The brownish powder was dissolved in acetonitrile and diethyl ether slowly diffused into the solution forming single-crystals suitable for X-ray analysis. The measurement was carried out on a STOE-IPDS diffractometer with graphite-monochromatised MoK α radiation. Table 3 summarises the crystal data, data collection, and refinement parameters. All calculations were performed with SHELX-97 package.^[24] The structure was solved by direct methods and was refined by full-matrix least-squares based on F^2 as an inversion twin. The (disordered) anions and hydrogen atoms were refined isotropically and with geometrical restraints. All hydrogen atoms were placed in calculated positions with $U(H) = 1.5 U_{eq}(C)$ for methyl groups and $U(H) = 1.2 U_{eq}(C)$ for all others.

X-ray crystallographic data for Co complex 4b · BF₄^{-M->}: Single crystals of complex **4b** (BF₄^{-M->} salt) were obtained in a cocrystallisation experiment with an Fe complex (not further characterised), which corresponded to Zn complex **12**. Compound **4** was dissolved in MeOH and an excess of NH₄BF₄ in MeOH was added. The precipitate was centrifuged and dried in vacuo, resulting a brown powder. Stoichiometric amounts of **4b** and the above mentioned Fe complex were dissolved in acetonitrile and diisopropyl ether slowly diffused into the solution to give two types of single crystals suitable for X-ray analysis. As the crystals proved to be too small for analysis with conventional X-ray equipment, measurements were carried out at beamline ID11 at the European Synchrotron Radiation Facility (ESRF). A wavelength of 0.5040 Å was selected with a double crystal Si(111) monochromator, and data were collected using a Bruker "Smart" CCD-

Table 3. X-ray data for complexes **4a**, **4b** and **12**.

	4a · PF ₆ ⁻	4b · BF ₄ ⁻	12
formula	C ₂₆ H ₂₂ CoN ₁₄ · 2 PF ₆ · 6 CH ₃ CN	C ₂₆ H ₂₂ CoN ₁₄ · 2.5 BF ₄ · 2.25 CH ₃ CN	C ₃₆ H ₄₂ N ₁₄ Zn · 2 CF ₃ SO ₃ · 2 CH ₃ CN · 0.5 C ₆ H ₁₄ O
<i>M</i> _r [g mol ⁻¹]	1125.73	898.87	1167.53
<i>T</i> [K]	200(1)	235(1)	173(2)
<i>λ</i> [Å]	0.71073	0.5040	0.71073
crystal system	orthorhombic	triclinic	monoclinic
space group	<i>Pna</i> 2 ₁	<i>P</i> $\bar{1}$	<i>P</i> 2 ₁ / <i>n</i>
<i>a</i> [Å]	16.015(2)	13.814(10)	14.0100(3)
<i>b</i> [Å]	19.671(5)	17.892(7)	18.6518(5)
<i>c</i> [Å]	15.641(2)	22.054(14)	22.4065(5)
<i>α</i> [°]	90	81.00(2)	90
<i>β</i> [°]	90	72.32(3)	92.261(1)
<i>γ</i> [°]	90	80.50(4)	90
<i>V</i> [Å ³]	4927.4(15)	5089(5)	5850.5(2)
<i>Z</i>	4	4	4
<i>ρ</i> _{calcd} [g cm ⁻³]	1.518	1.240	1.326
<i>μ</i> (MoK α) [mm ⁻¹]	0.512	0.222	0.568
<i>F</i> (000)	2292	1930	2420
crystal size [mm]	0.15 × 0.15 × 0.10	0.08 × 0.05 × 0.03	0.4 × 0.4 × 0.3
<i>θ</i> range [°]	1.64–24.04	8.05–15.38	2.94–27.97
index ranges	–18 ≤ <i>h</i> ≤ 18 –10 ≤ <i>k</i> ≤ 21 –16 ≤ <i>l</i> ≤ 17	–14 ≤ <i>h</i> ≤ 13 –15 ≤ <i>k</i> ≤ 18 –23 ≤ <i>l</i> ≤ 22	0 ≤ <i>h</i> ≤ 18 –24 ≤ <i>k</i> ≤ 24 –29 ≤ <i>l</i> ≤ 29
reflections collected	11832	16035	35407
<i>R</i> (int)	0.0861	0.0746	0.0582
independent reflections	6384	9830	13933
data/restraints/parameters	6384/718/668	9830/986/1128	13933/55/676
GoF	0.978	1.038	0.896
final <i>R</i> indices [<i>I</i> > 2σ(<i>I</i>)]	<i>R</i> ₁ = 0.0725 <i>wR</i> ₂ = 0.1737	<i>R</i> ₁ = 0.0826 <i>wR</i> ₂ = 0.2040	<i>R</i> ₁ = 0.1123 <i>wR</i> ₂ = 0.3190
<i>R</i> indices (all data)	<i>R</i> ₁ = 0.1263 <i>wR</i> ₂ = 0.2079	<i>R</i> ₁ = 0.1068 <i>wR</i> ₂ = 0.2190	<i>R</i> ₁ = 0.1704 <i>wR</i> ₂ = 0.3828
largest diff. peak/hole [e Å ⁻³]	0.387/–0.325	0.46/–0.39	1.198/–0.890

camera system at fixed 2θ , while the sample was rotated over 0.1° intervals during 2 s exposures. Data were reduced with the Bruker SAINT software. Structure solution by direct methods and refinement on F^2 were carried out with SHELX-97.^[24] Details of the data collection and analysis are summarised in Table 3. The structure contains seven intercalated acetonitrile molecules per asymmetric unit. Hydrogen atoms were placed in idealised positions and their isotropic temperature parameters were fixed with respect to those of the atoms they ride upon. Further geometrical and thermal factor constraints were introduced in order to stabilise a reasonable structure for the anions.

X-ray crystallographic data for Zn complex 12: A suitable yellowish crystal of [C₃₆H₄₂N₁₄Zn]²⁺ · 2 CF₃SO₃⁻ · 2 CH₃CN · 0.5 C₆H₁₄O was obtained from deuterio acetonitrile/diisopropyl ether. Data were recorded with a Nonius Kappa CCD diffractometer, with 258 frames, each frame covering an 1° oscillation with an exposure time of 2×15 s. Table 3 summarises the crystal data, data collection, and refinement parameters. The data were processed with *Denzo*.^[25] The absorption correction was made with SORTAV,^[26] but not applied. *L_p* correction was applied. Structure solution was done by direct methods and refinement on F^2 . The hydrogen atoms were calculated to their idealised positions with isotropic temperature factors (1.2 or 1.5 times the C temperature factor) and were refined as riding atoms. 55 geometrical DFIX restraints were needed to make one of the alkyl chains, the triflate anions, one acetonitrile and diisopropyl ether chemically reasonable. In both triflate anions carbon, fluorine and oxygen atoms were disordered over two orientations with the site occupation values of 0.60 and 0.40 for one and 0.70 and 0.30 for another triflate. An acetonitrile molecule was disordered between two positions with the population parameters of 0.47 and 0.53. The diisopropyl ether molecule was treated with occupancy of 0.5. Altogether 45 temperature factors were equalised by EADP constraints. A final difference map displayed the highest electron density of 1.20 e Å⁻³, which is located near to disordered triflate anions.

Crystallographic data (excluding structure factors) for the structures reported in this paper have been deposited with the Cambridge Crystallo-

graphic Data Centre as supplementary publication no. CCDC-143708 (**4a**), CCDC-143709 (**4b**) and CCDC-143711 (**12**). Copies of the data can be obtained free of charge on application to CCDC, 12 Union Road, Cambridge CB21EZ, UK (fax: (+44)1223-336-033; e-mail: deposit@ccdc.cam.ac.uk).

Acknowledgements

U.Z. thanks the Deutsche Forschungsgemeinschaft for a postdoctoral fellowship. E.B. thanks the French Government for an undergraduate fellowship and the Ministère de l'Éducation Nationale, de la Recherche et de la Technologie for a postgraduate fellowship. Financial support from the Finnish Ministry of Education is gratefully acknowledged by E.W. We thank Dr. Jean-Paul Gisselbrecht for the electrochemical investigations. We thank Dr. Mubarak Chowdhry for his assistance with the crystal mounting and synchrotron X-ray measurements. We thank the ESRF for provision of beam time.

- [1] a) J.-M. Lehn, *Supramolecular Chemistry: Concepts and Perspectives*, VCH, Weinheim, **1995**; b) *Comprehensive Supramolecular Chemistry, Vol. 9* (Eds: J. L. Atwood, J. E. D. Davies, D. D. MacNicol, F. Vögtle, J.-M. Lehn), Pergamon, New York, **1996**.
- [2] D. Braga, F. Grepioni, *J. Chem. Soc. Dalton Trans.* **1999**, 1–8.
- [3] C. B. Aakeröy, A. M. Beatty, *Chem. Commun.* **1998**, 1067–1068.
- [4] C. B. Aakeröy, A. M. Beatty, D. S. Leinen, *Angew. Chem.* **1999**, *111*, 1932–1936; *Angew. Chem. Int. Ed.* **1999**, *38*, 1815–1819.
- [5] Z. Qin, H. A. Jenkins, S. J. Coles, K. W. Muir, R. J. Puddephatt, *Can. J. Chem.* **1999**, *77*, 155–157.
- [6] C. Janiak, S. Deblon, H.-P. Wu, M. J. Kolm, P. Klüfers, H. Piotrowski, P. Mayer, *Eur. J. Inorg. Chem.* **1999**, 1507–1521.

- [7] A. D. Burrows, C.-W. Chan, M. M. Chowdry, J. E. McGrady, D. M. P. Mingos, *Chem. Soc. Rev.* **1995**, 329–339.
- [8] M. Tadokoro, K. Isobe, H. Uekusa, Y. Ohashi, J. Toyoda, K. Tashiro, K. Nakasuji, *Angew. Chem.* **1999**, *111*, 102–106; *Angew. Chem. Int. Ed.* **1999**, *38*, 95–98.
- [9] B. Lippert, P. Amo-Ochoa, W. Brüning, E. Freisinger, M.-S. Lüth, S. Meier, C. Meiser, S. Metzger, H. Rauter, A. Schreiber, R. K. O. Sigel, H. Witkowski, *Pure Appl. Chem.* **1998**, *70*, 977–983.
- [10] M. Lounasmaa, C.-J. Johansson, *Tetrahedron* **1977**, *33*, 113–117.
- [11] O. Isler, H. Gutmann, O. Straub, B. Fust, E. Böhni, A. Studer, *Helv. Chim. Acta* **1955**, *38*, 1033–1046.
- [12] M. L. Scudder, H. A. Goodwin, I. G. Dance, *New J. Chem.* **1999**, *23*, 695–705.
- [13] B. Whittle, E. L. Horwood, L. H. Rees, S. R. Batten, J. C. Jeffery, M. D. Ward, *Polyhedron* **1998**, *17*, 373–379.
- [14] W. Henke, S. Kremer, *Inorg. Chim. Acta* **1982**, *65*, L115–L117.
- [15] I. S. A. Farag, A. M. Gad, A. M. El-Shabiny, V. B. Rybakov, *Cryst. Res. Technol.* **1993**, *28*, 1127–1133.
- [16] C. J. B. Clews, W. Cochran, *Acta Crystallogr.* **1949**, *2*, 46–57.
- [17] B. N. Figgis, S. Kucharski, A. H. White, *Aust. J. Chem.* **1983**, *36*, 1563–1571.
- [18] R. Prasad, D. B. Scaife, *J. Electroanal. Chem.* **1977**, *84*, 373–386.
- [19] M. Chao, E. Schempp, R. D. Rosenstein, *Acta Crystallogr. Sect. B* **1976**, *32*, 288–290.
- [20] D. J. Brown, J. S. Harper, *J. Chem. Soc.* **1961**, 1298–1303.
- [21] L. Crombie, R. C. F. Jones, C. J. Palmer, *J. Chem. Soc. Perkin Trans. I* **1987**, 317–331.
- [22] N. Sato, *J. Heterocycl. Chem.* **1982**, *19*, 673–674.
- [23] M. Benaglia, S. Toyota, C. R. Woods, J. S. Siegel, *Tetrahedron Lett.* **1997**, *38*, 4737–4740.
- [24] G. M. Sheldrick, *SHELX-97*, Universität Göttingen, **1997**.
- [25] Z. Otwinowski, W. Minor, *Methods in Enzymology*, Vol. 276 (Eds: C. W. Carter Jr., R. M. Sweet), Academic Press, **1997**.
- [26] R. H. Blessing, *Acta Crystallogr. Sect. A* **1995**, *51*, 33–37.

Received: May 8, 2000 [F2468]